Effect of Calcination Kinetics and Microwave Sintering Parameters on Dielectric and Pieizo-Electric Properties of ($K_{0.5}Na_{0.5}$) NBO_3 Ceramics

R. N. Nandini[1], M. Krishna[1*], A. V. Suresh[2] and K. Narasimha Rao[3]

* *krishnam@rvce.edu.in*

Received: September 2017 Accepted: February 2018

[1] Department of Mechanical Engineering, R.V. College of Engineering, Bangalore, India.
[2] Department of Mechanical Engineering, BMS Institute of Technology, Bangalore, India.
[3] Department of Instrumentation and Applied Physics, Indian Institute of science, Bangalore, India.
DOI: 10.22068/ijmse.15.2.14

Abstract: *An efficient solid-state approach was established to synthesize ($K_{0.5}Na_{0.5}$) NbO_3 ceramics using calcination kinetics and microwave assisted sintering. Milling of carbonate and oxide raw materials were carried out for 15 h to obtain homogeneous nano particles. The crystallite size of 5.30 nm was obtained for the KNN system after calcination through optimized parameters and observed to be stoichiometric in nature. The obtained nano particles showed phase transition from orthorhombic to tetragonal crystal structure without any secondary phases. The high relative density and tetragonality ratio of KNN ceramics obtained through optimized sintering parameters yielded with significant piezoelectric and ferroelectric properties.*

Keywords: *KNN, Solid state method, Calcination kinetics, Microwave Sintering, Piezo-electric properties.*

1. INTRODUCTION

An intense research on lead free piezo-electric ceramics is being carried out worldwide for more than a decade due to environmental concern and toxicity of lead-based ceramics [1-2]. Investigation based on alkali niobates ($ANbO_3$) has gained momentum in recent times. The general form of these lead-free perovskite materials is $ANbO_3$ [3]. Potassium niobates ($KNbO_3$) exhibited greater piezo-electric properties, which are stable along the non-polar crystallographic directions than along the polar axis and exhibits stable orthorhombic phase over a wide temperature range [4-6]. It has high piezo-electric coefficient among the lead free based piezo materials. $KNbO_3$ is extensively used in amalgamation with sodium niobates ($NaNbO_3$) as a binary system which makes it one of the most promising lead-free piezoelectric materials. It is a combination of ferroelectric (FE), $KNbO_3$ and an anti-ferroelectric (AFE) $NaNbO_3$. Ferro-electricity is reported to be up to 90% in $KNbO_3$ in the binary system of $KNbO_3$-$NaNbO_3$[7]. Based on a study on various stoichiometric ratios, it was observed that the composition $K_{0.5}Na_{0.5}NbO_3$ (KNN) was favorable, and the composition (50/50) is in between two orthorhombic phases at morphotropic phase boundary (MPB) as observed in lead zirconate titanate (PZT) [8]. Potassium sodium niobate (KNN) is satisfactorily recommended for a broad range of applications due to its high Curie temperature (Tc) of 420 °C and a low density of 4.51 g/cm^3[9].

The Conventional solid-state route, wet chemistry methods such as sol-gel, hydrothermal has been applied for synthesis of KNN nano-size powders [10-13]. Sol-gel and solid-state synthesis of KNN ceramics have drawn much interest due to its ability to obtain nano-size powders. The hydrated carbonated phases formed during sol-gel process needs high temperature (near melting point ~1140 °C) to decompose and this increases the volatile behavior of alkaline elements of KNN [11,12]. The use of soft chemistry though reduced the synthesis temperature overcoming volatile behavior of alkaline elements but could not avoid the presence of carbonates during heat treatment, there by showing the need for high temperature [11,12]. Since solid state route can easily decompose oxides and carbonates, it is extensively used to synthesize ferroelectric

[DOI: 10.22068/ijmse.15.2.14]

powders for good control on particle morphology [11]. Microwave assisted sintering of KNN ceramics at 1115 °C achieved peizo-electric charge co-efficient (d_{33}) value of 85 pC/N and P_r of 18 μC/cm² with 93.8 % bulk density [14]. However only 3 % of the total conventional sintering time (16 h) reported to obtain d_{33} value of 80-160 pC/N was needed in case of microwave sintering [20-21]. Microwave sintered samples observed to be more in dense, fine uniform microstructure and 50 % increase in d_{33} value [17]. KNN samples prepared by spark plasma sintering (SPS) method at 920 °C exhibited d_{33} value of 148 pC/N and k_p of 0.389 [18]. SPS sintered samples exhibited high coercive field, dielectric constant at room temperature and low remnant polarization [18]. But the smaller grain size obtained by SPS method needs post annealing of the samples to obtain better d_{33} values [21]. Post annealing is also associated with secondary grain growth which effects the densification and functional properties [19-22]. Overall microwave assisted sintering is the best route to fabricate KNN ceramics in a short time with improved piezo-electric properties. But in KNN ceramics, the presence of one more phase transformation around 200 °C makes it less useful and needs further research [23]. Moreover, volatile nature of alkaline elements, phase instability of KNN at high temperature and low relative density of sintered body results in difficulty to synthesize KNN ceramics, with high densification and good piezo-electric properties.

Hence there is a need to analyze the kinetics behind the reaction mechanism of KNN particles. The solid-state kinetics helps in achieving completion of the reaction mechanism successfully without secondary phases, thereby reducing volatility nature of alkaline elements and improving its densification and peizo-electric properties.

In the present work, $(K_{0.5}Na_{0.5})$ NbO_3 system was synthesized using solid-state route by establishing the calcination kinetic parameters to overcome volatile nature and phase instability of alkaline elements. Calcined powders were compacted and densified using unidirectional pressing and microwave assisted sintering. Later the densified KNN ceramics were characterized structurally and functionally to evaluate physical, chemical, piezo-electric and ferroelectric properties of KNN peizo-electric ceramics.

2. EXPERIMENTAL PROCEDURE

The materials Na_2CO_3 (≥ 99.5 %), K_2CO_3 (≥99.0 %), and Nb_2O_5 (99.9%) were used as supplied by Alpha Aesar, UK. The measured stoichiometric mixtures for the system $(K_{0.5}Na_{0.5})$ NbO_3, (KNN) were preheated at 200 °C for 2 h. This preheated mixture was blended in high energy planetary ball mill PM 200 (Retsch GmbH) for 15 h at 300 rpm using 2.5 ml of acetone as processing medium. Stainless steel balls were used to mix the powder with ball to powder ratio (BPR) of 10:1. Each cycle corresponded to 2 h of milling up to completion of 14 h and 1 h cycle for last milling hour. After each cycle, the steel vial was cleaned and 0.2-0.5 ml of acetone was added as a processing agent to avoid adhesion of the powder with vial wall. The blended powder of KNN was calcined at the temperature of 700, 800 and 900 °C for different time intervals of 7, 8 and 10 h in the conventional furnace.

The process helps to complete solid state reaction and obtain required $(K_{0.5}Na_{0.5})$ NbO_3 system by establishing calcination parameters. The thermal degradation of mixed raw powder and the effect of calcination process parameters on crystal structure, microstructure and transmittance of KNN powder were analyzed using thermo gravimetry / differential thermal analyzer (DTG-60, Shimadzu), X-ray diffractometer (XRD, Rigaku Smart Lab), Fourier Transform Infrared Spectroscopy (FT/IR – 4200, Jasco Germany), and scanning electron microscopy (SEM, Zeiss Supra-40) respectively. The diffractometer was used with Cu-K_α monochromatic radiation for the range of 2Θ values from 10 - 80°. The crystallite size of calcined KNN powder was computed using Scherer's equation Eq. (1) (Instrumental broadening of the system used for correction of the data):

$$\boldsymbol{D = \frac{k * \lambda}{B * cos\theta}} \quad (1)$$

where D-crystallite size, k = 0.89 (Scherer's constant), λ-wavelength(X-ray), B- full width at half maximum of the diffraction peak, and Θ-angle of diffraction. The FTIR spectroscopy was carried out from 400 cm^{-1} to 4000 cm^{-1} to

[DOI: 10.22068/ijmse.15.2.14]

determine the transmittance. The thermal degradation was carried out using DTG - 60 with a heating rate of 2 °C /min from RT to 900 °C in inert atmosphere with N_2 gas flow rate of 50 ml/min. The grain size and morphology of calcined powders were evaluated using transmission electron microscopy (TEM, Philips CM 200 FEGTEM) with 200 kV accelerating voltage and SEM (Zeiss Supra-40) operating at 20 kV respectively. The synthesized KNN powder were milled again for 1 h to overcome the agglomerations formed during calcination process and pressed uniaxially at 250 MPa using universal testing machine to obtain disc of 10 mm diameter with ~ 1.5 mm thickness.

These green compacts were sintered using 1600 AC microwave furnace, Super (VBCC, Chennai) at temperature of 1100 °C, for a duration of 30 min to get densified samples. The relative density of the sintered bodies was determined by Archimedes principal using density meter. KNN sintered samples were polished using silicon carbide powder to obtain required aspect ratio. The prepared KNN samples were given electrical contacts by using high temperature silver paste. Semiconducting device analyzer B1500A was used to measure capacitance, impedance and dissipation factor of KNN sintered sample between ranges from 1 kHz to 1 MHz.

$$\varepsilon_r = \frac{(C*t)}{(\varepsilon_o * A)} \qquad (2)$$

Dielectric constant (ε_r) was evaluated from room temperature to 450°C using Eq. 2. Where C is capacitance measured, t- sample thickness, A- surface area of the sample and $\varepsilon_\circ$ - permittivity of the free space (8.54×10^{-12} F/m). The electromechanical coupling co-efficient (K_p) of sintered KNN ceramics was evaluated using Eq. 3. Where K_p is the planar mode coupling factor, f_r - resonance frequency (impedance is minimum) and f_a - anti resonance frequency (impedance is maximum).

$$K_P^2 = 2.51 \frac{(f_a - f_r)}{f_r} \qquad (3)$$

$$Q_m = \frac{1}{2\pi f_r RC}\left\{\frac{f_a^2}{f_a^2 - f_r^2}\right\} \qquad (4)$$

The mechanical quality factor (Q_m) was determined by Eq. 4. R and C are the resonance-impedance and capacitance respectively at 1 kHz. The peizo-electric charge coefficient (d_{33}) was measured under a field of 4 kV/mm for 30 min at 100 °C by Piezotest PM 300 Piezotest Pte. Ltd, Singapore. The hysteresis loops were determined by using precision premier II ferroelectric tester (Radiant technologies. INC) at room temperature under 5 kV/mm, AC field at 50 Hz with a unit, based on modified sawyer-tower circuit [14].

3. RESULTS AND DISCUSSION

Fig. 1 indicates X-ray diffraction pattern of initial and mixed raw powder of KNN at 5 h ,10 h and 15h. The XRD pattern of initial raw mixture reports many minor peaks which are attributed to the heterogeneous nature due to presence of the starting materials (K_2CO_3, Na_2CO_3, Nb_2O_5) as reported in Fig. 1. The diffraction pattern of 5h mixed raw powder initiates formation of the perovskite structure at 22.21° and 75.59° with few minor peaks associated with the remains of initial mixture, thereby arising the need for further milling. In addition, the 10h milled raw powder showed improved intensity of the perovskite peaks at 22.42° ,28.22° and 72.59° with reduced intensity of

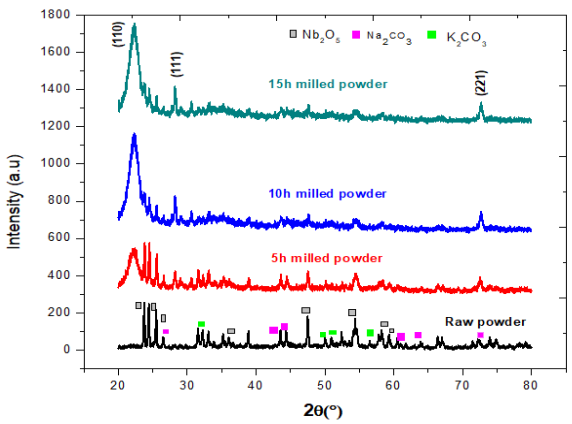

Fig. 1. XRD patterns of initial and mixed raw powders of KNN

[DOI: 10.22068/ijmse.15.2.14]

minor peaks between 45-55°, which may be attributed to the disappearance of the remains of initial mixture.

Further, the diffraction pattern of 15 h mixed powder was similar to that of 10 h milled powder. It can be attributed to formation of homogenous blended KNN powder. Furthermore, there was improvement in the intensity of orthorhombic crystal structure of KNN at 110, 111 and 221 planes as shown in Fig. 1. for 15h of milling. Hence, 15h mixing time is considered to be the optimized milling duration to obtain nano-crystalline homogenous KNN powder.

The solid-state reaction between the starting precursors was analyzed using thermal analysis as shown in Fig. 2. The DTA curve shows a pronounced exothermic peak at 145.74 °C and 504.10°C which indicates that the DTA peak corresponds to the reaction between the alkali carbonates and the Nb_2O_5 [26]. According to the TG curve, the weight loss of KNN mixture in the temperature ranges 96 °C - 536.59 °C, 536.59 °C-723.51°C and 96°C - 723.51 °C are 13.69%, 2.913% and 16.60% respectively. The weight loss peak at 197.29 °C is attributed to simultaneous losses of H_2O and CO_2[24].

The decomposition of carbonates [$AHCO_3$] into bi-carbonates [A_2CO_3], where A is associated with K^+ and Na^+ ions occurs between 96.89 ° and 197.29 °C [25]. The first exothermic peak at 145.74 °C is due to reaction between alkaline carbonates and niobium oxide. The second endothermic peak at 504.10 °C, based on diffusion study [27] corresponds to the formation of an intermediate reaction layer of $(K, Na)_2 Nb_4O_{11}$[16] on the surface of Nb_2O_5 particles. Further development of the reaction at 735.44 °C leads to the formation of a stoichiometric $(K_{0.5}Na_{0.5}) NbO_3$ phase at the surface of the reaction layer. The maximum weight loss peaks at 455.25 °C and 536.59 °C corresponds to coupled diffusion reaction between K+, Na+, O+ ions into niobium oxide with the removal of CO_2 gas [27]. The complete decomposition of carbonates was observed at 723 °C. Based on thermal stability of KNN powder, calcination treatment was selected at 723 °C and above to establish its parameters.

The diffraction patterns of calcined KNN powders (700, 800 and 900 °C) for duration of 5, 7 and 10 h are given in Fig. 3(a), 3(b) and 3(c) respectively. KNN powders calcined at 700 °C reveals the formation of perovskite crystal structure (JCPDF # :01-077-0037) at 2Θ values between 20-35 ° at (111) and (100) plane with an initiation for formation of single perovskite structure at (200), (202) and (222) planes between 45- 60 ° as given in Fig. 3(a). The intensity of the perovskite structure at

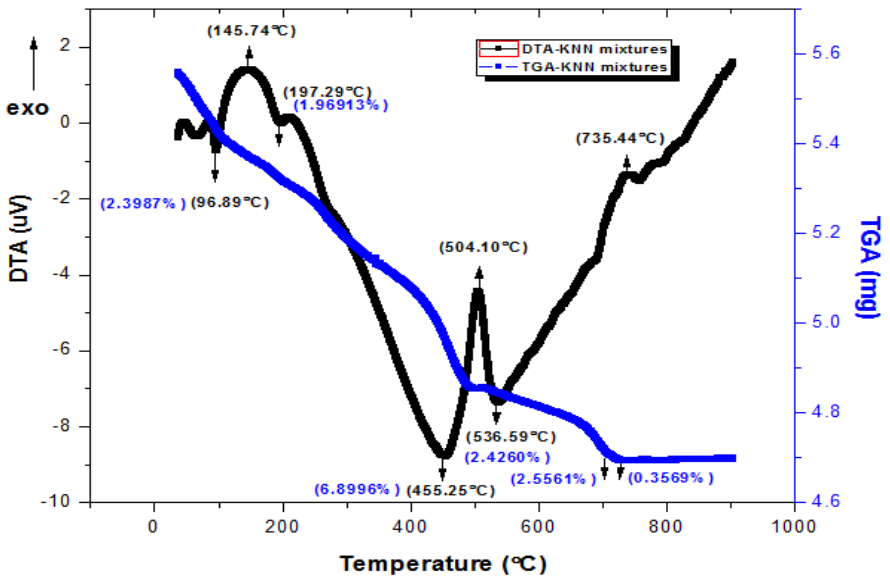

Fig. 2. TGA and DTA curves of the KNN mixtures.

[DOI: 10.22068/ijmse.15.2.14]

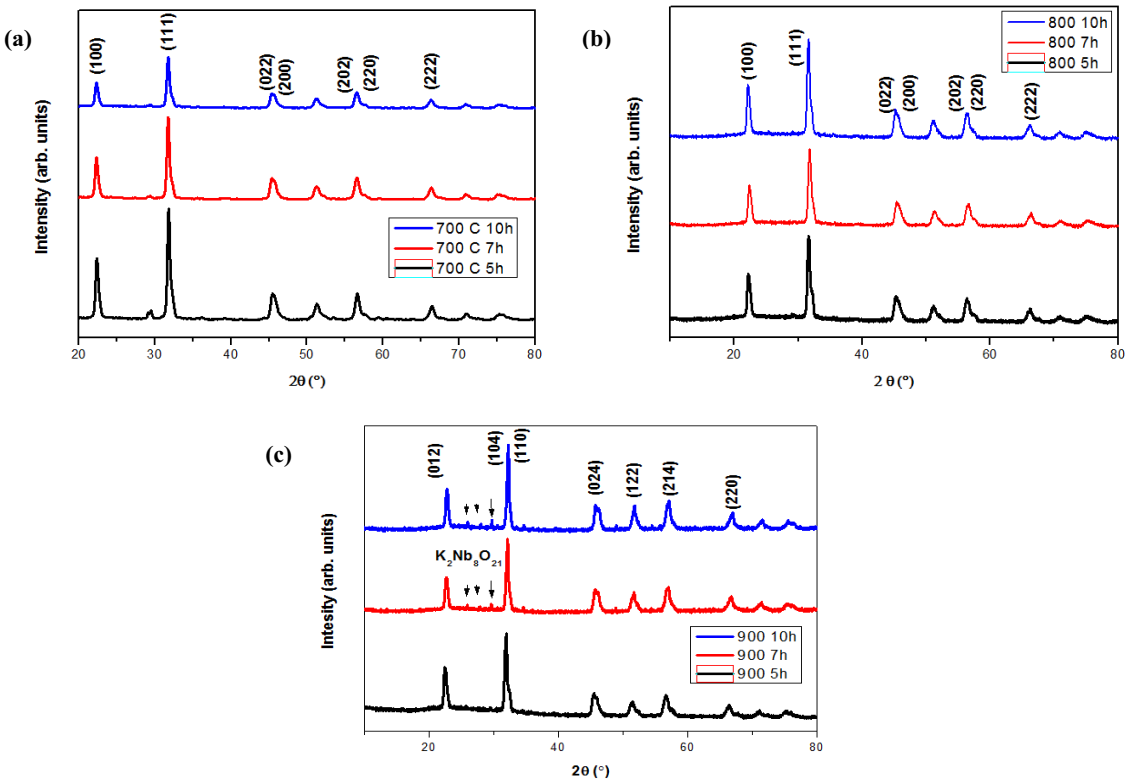

Fig. 3. XRD patterns of calcined KNN powders at temperature of a) 700 °C, b) 800 °C and c) 900 °C.

20-35°for 800 °C calcined powders (Fig. 3(b)) showed prominent peaks at the planes (100) and (111) with an improved intensity of some peaks, specially at 2Θ = 45-60 °C, which indicates formation of single phase orthorhombic perovskite crystal structure. Complete growth of pure orthorhombic structure at (100) and (111) plane was observed in 900 °C calcined powders (Fig. 3(c)) between 20-35°. The prominent peak split up between 45-47° at (024) plane and improved peak intensity between 50-60° at (122) and (214) planes in (Fig. 3(c)) indicates complete formation of single phase orthorhombic crystal structure [16]. Diffraction pattern for KNN powders calcined at temperature of 900 °C for duration of 5 h (Fig. 3(c)) revealed pure orthorhombic structure without formation of complex oxides. However, there were a few complex oxides (secondary phases) formed by $K_2Nb_8O_{21}$(JCPDF #:031-1060) at 900 °C, of 7 h and 10h calcined powders. Hence the optimized calcination parameter to synthesize ($K_{0.5}Na_{0.5}$) NbO_3 powders was 900 °C, 5 h.

Fig. 4 shows the effect of calcination temperature and duration on the crystallite size of KNN powder. The crystallite size increased continuously from 9.47 ± 0.1 nm to 9.74 ± 0.12 nm for KNN powder calcined at temperature of 700 °C for different time periods. However, the increase in crystallite size is much higher for the durations beyond 7 h. Whereas the growth of the KNN crystallite size for 800 °C calcined powder was increased gradually from 12 ± 0.11 to 12.45 ± 0.12 nm with duration. However, the variation in the crystallite size between 7 and 10h was comparatively less, indicating 90% completion of the solid-state reaction. The crystallite size of KNN powder calcined at 900 °C ranged from 13.04 ± 0.13 to 13.78 ± 0.13 nm. The increase in crystallite size is negligible for KNN calcined powder at 900 °C for 7h and 10h. This shows the completion of solid state reaction and is in agreement with previously derived kinetic models [37].

The FTIR spectrum of KNN mixture and calcined KNN powders at different temperature identifies the functional groups and the formation of pure

[DOI: 10.22068/ijmse.15.2.14]

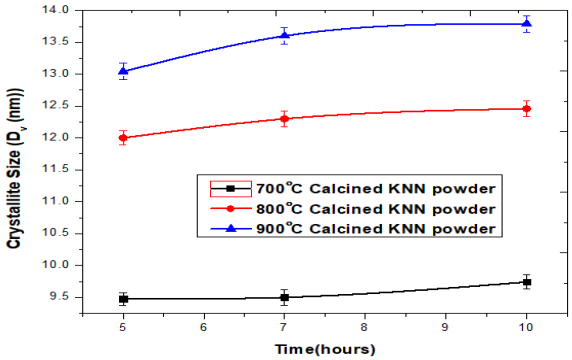

Fig. 4. Crystallite size of KNN powders as a function of time for temperatures calcined at 700 °C, 800 °C and 900 °C.

compound between 1800 and 500 cm^{-1} as shown in Fig. 5(a) and 5(b) respectively. Fig. 5(a) depicts the absorption bands at 1638.56 cm^{-1}, 1446.05 cm^{-1}, 847.01cm^{-1} and 670.33 cm^{-1} associated with vibrations of H_2O [18], C-O stretching, deformation of carbonate group (CO32-) and vibrations of (Nb5+ cations), B-O groups respectively [16]. Curve 1 of Fig. 5(b) i.e. 700 °C calcined powder, shows the formation of perovskite structure at 654.16 cm^{-1} with reduced absorbent bands at 1667.19 cm^{-1}, 1458.18 cm^{-1} ensuring completion of C-O stretch band and partial removal of H_2O content. But the transmittance spectrum of samples at 800°C and 900 °C revealed single broad penetration band at 680 cm^{-1} due to the formation of perovskite phase [28] indicating that it is a single oxide functional group of

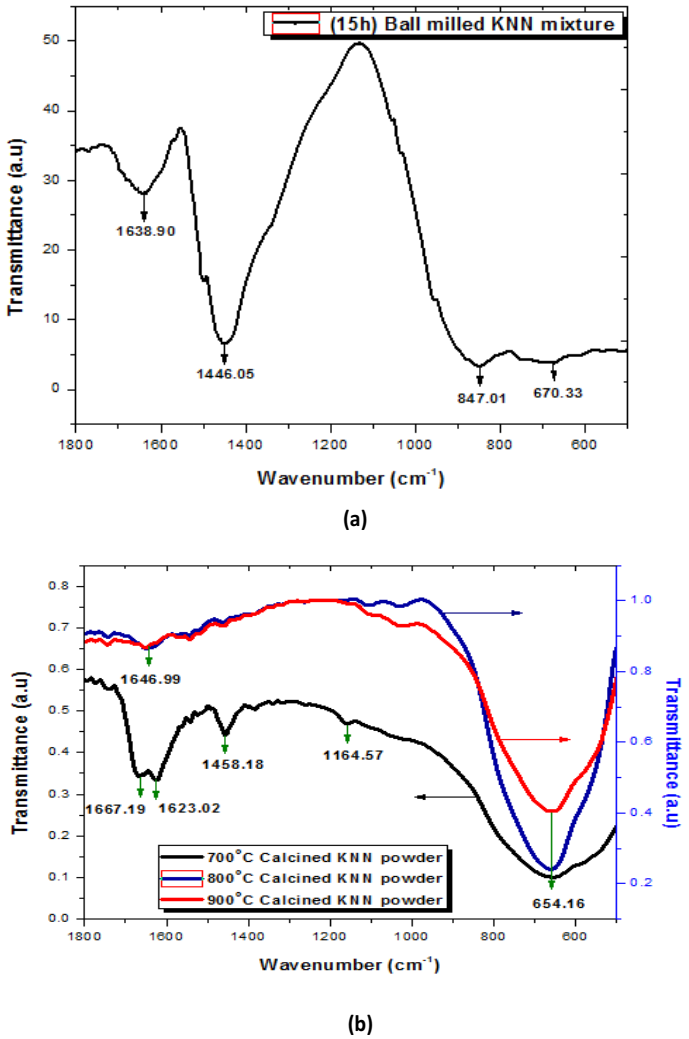

Fig. 5. FTIR spectra of (a) KNN mixture and (b) Calcined KNN powders.

[DOI: 10.22068/ijmse.15.2.14]

Na-O-K. These are in agreement with the TGA/DTA results (Fig. 2), where the decomposition of carbonates was complete for KNN samples at ~700 °C with no further weight loss.

The morphology of KNN powder calcined at 700, 800 and 900 °C for 5h reported cubical crystal structure is as shown in Fig. 6(a), 6(b) and 6(c) respectively. The particles at 700 °C calcined powders were not densely packed and the presence of voids between the particles indicated that the solid-state reaction of KNN powder were still in progress. Whereas 800 °C calcined powders showed reduced voids with better compactness among the particles attributing to almost (90%) completion of the reaction. However, the particles in 900 °C calcined powders (Fig. 6(c)) were densely packed without voids due to the completion of the reaction which were in agreement with TG-DTA results (Fig. 2). The size of the particles as measured from micrographs is in the range 54.57nm - 195.3 nm and few agglomerates 257-300 nm in size were formed by these particles as observed by others [13]. TEM micrographs of calcined KNN powders at 900 °C for 5 h is shown by Fig. 7(a) lower magnification and 7(b) higher magnification. The average grain size of calcined KNN powder obtained by Image J analysis was 5.30 nm, which is comparatively lesser than computed grain size by Scherer's equation (Fig. 4).

EDS analysis of calcined KNN particles at different temperatures are shown in Figs. 8(a), 8(b) and 8(c). The presence of carbon and oxygen element peaks at 700 °C (Fig. 8(a)), and 800 °C (Fig. 8(b)), calcined samples indicate that solid state reaction is not completed. These are in agreement with Table 1 and Table 2 respectively. For samples processed at 900 °C (Figs. 8(c)), the intensity of these elements (C, O) were negligibly small and were mapping with Table 3, which indicated that reaction of KNN calcined powders were completed. The presence of niobium rich peaks and associated potassium and sodium ions (Fig. 8(a) and 8(b)) indicates the existence of required system. However, the sample processed at 900 °C (Figs. 8(c)) shows reduced peak intensity for niobium ion and this may be due to the diffusion of niobium ions into potassium and

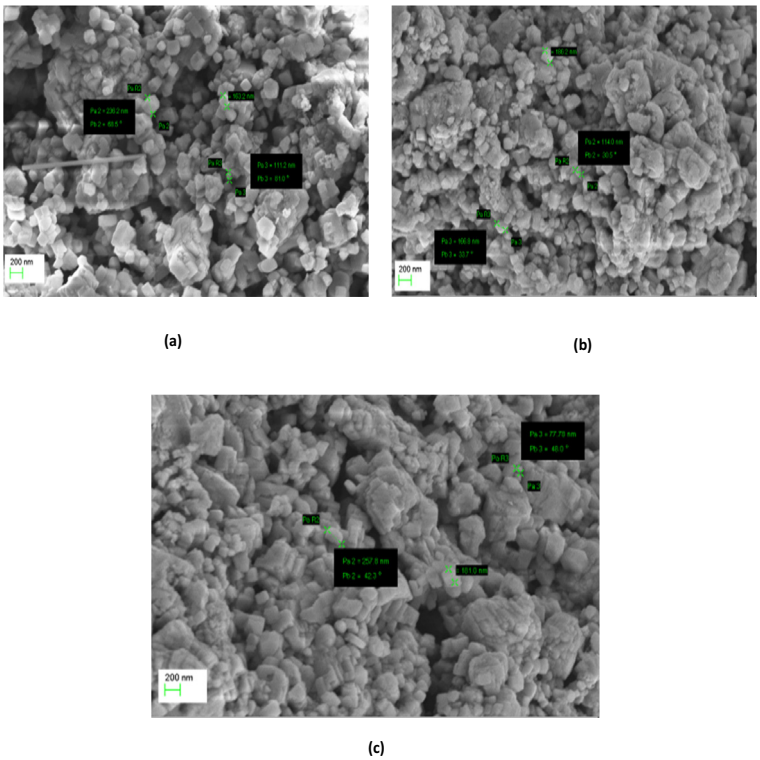

Fig. 6. Micrographs of KNN powders calcined at temperatures (a) 700 °C (b)800 °C and (c) 900 °C.

[DOI: 10.22068/ijmse.15.2.14]

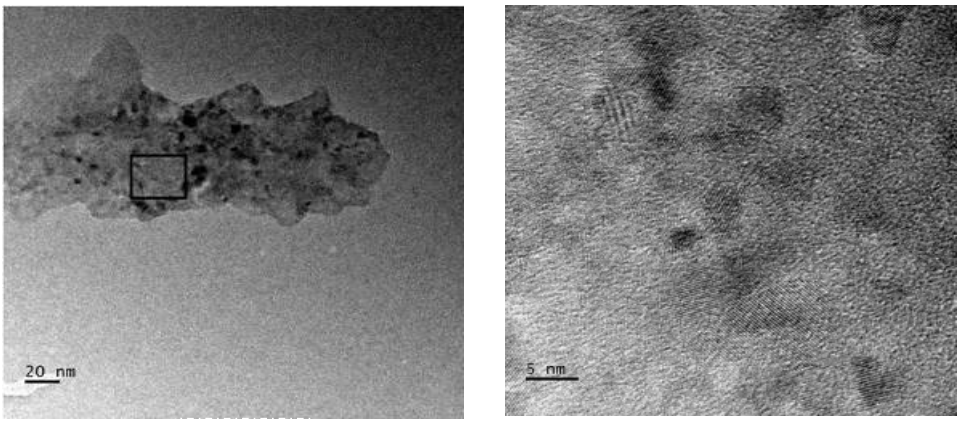

Fig. 7. Transmission electron micrographs of KNN powders calcined at 900 °C for 5h, at lower magnification (a) 20nm and higher magnification (b) 5nm.

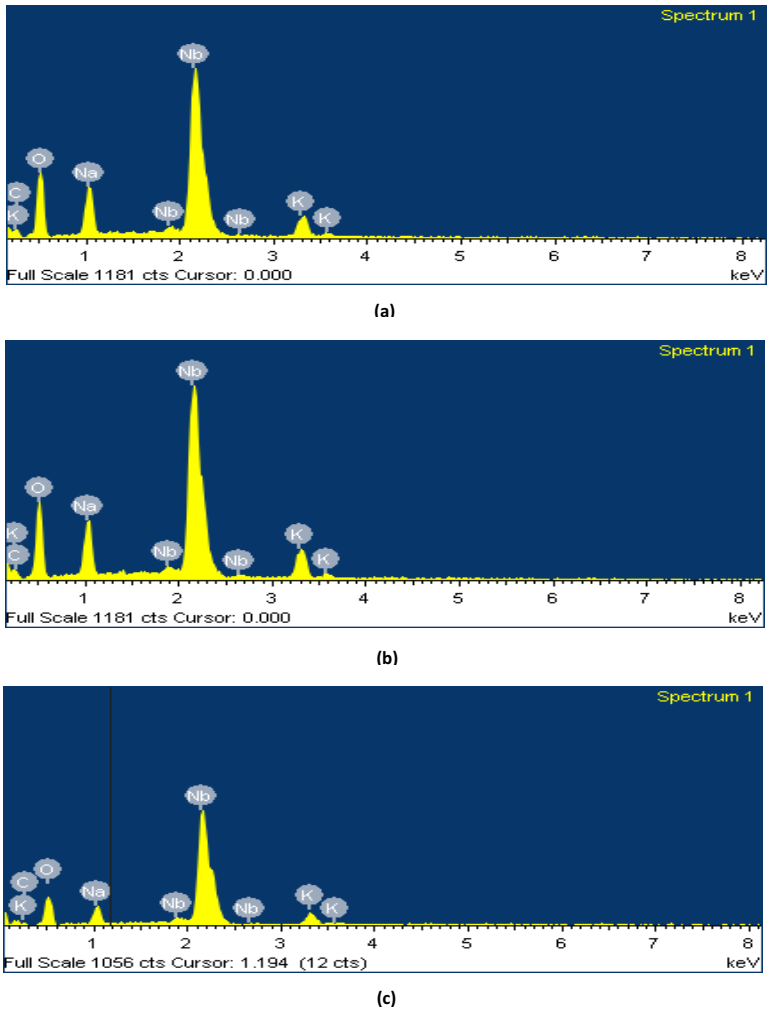

Fig. 8. EDS spectra of a KNN powders calcined at (a) 700 (b) 800 and (c) 900 °C for 10h.

[DOI: 10.22068/ijmse.15.2.14]

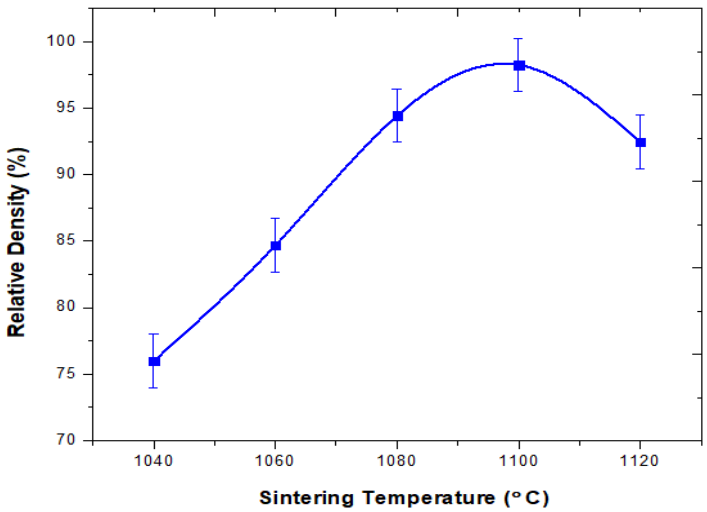

Fig. 9. Relative density of KNN Ceramics as a function of sintering temperature.

sodium ions to obtain $(K_{0.5}Na_{0.5})$ NbO_3 system.

The relative density of KNN ceramics, microwave sintered at different temperatures is shown in Fig. 9. The relative density of the sintered samples increased linearly with the increase of temperature up-to 1100 °C. Further the samples sintered at 1100 °C for 30min yielded with 98±2 % relative density. However, the samples sintered at 1120 °C near to its melting point (1140 °C) resulted in reduced relative density of 95±2 %. Hence the optimized sintering temperature was 1100 °C to obtain densified samples. The weight loss in sintered samples at 1100 °C was negligible, signifying reduced volatility of alkaline materials in

Table 1. Elemental Table of KNN powder calcined at 700 °C, 10 h.

Element	Weight%	Atomic%
C K	6.49	15.70
O K	31.12	56.53
Na K	6.16	7.79
K K	5.57	4.14
Nb L	50.65	15.84
Totals	100.00	

Table 2. Elemental Table of KNN powder calcined at 800 °C ,10 h.

Element	Weight%	Atomic%
C K	5.48	13.35
O K	32.25	58.93
Na K	6.35	8.08
K K	4.71	3.52
Nb L	51.21	16.12
Totals	100	

Table 3. Elemental Table of KNN powder calcined at 900°C ,10 h.

Element	Weight%	Atomic%
C K	0.00	0.00
O K	27.69	63.39
Na K	4.51	7.19
K K	4.96	4.64
Nb L	62.84	24.78
Totals	100.00	

[DOI: 10.22068/ijmse.15.2.14]

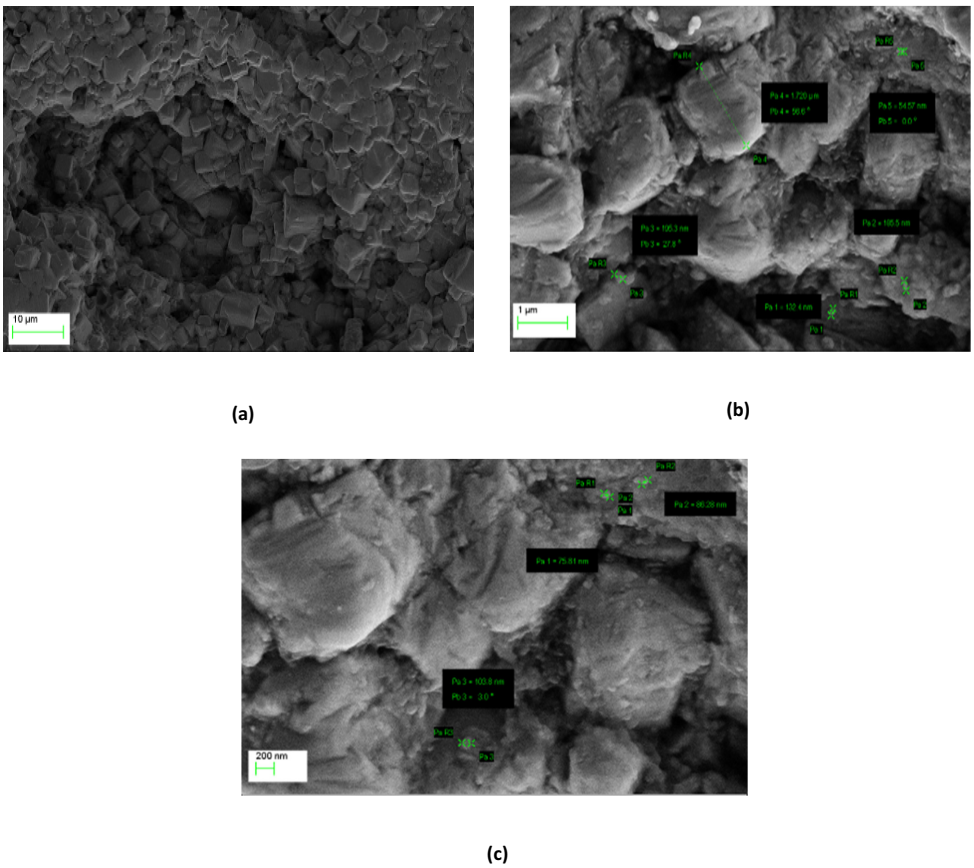

Fig.10. Micrographs of microwave assisted sintered KNN samples at 1100 °C at 30 min for different magnifications (a), (b) and (c).

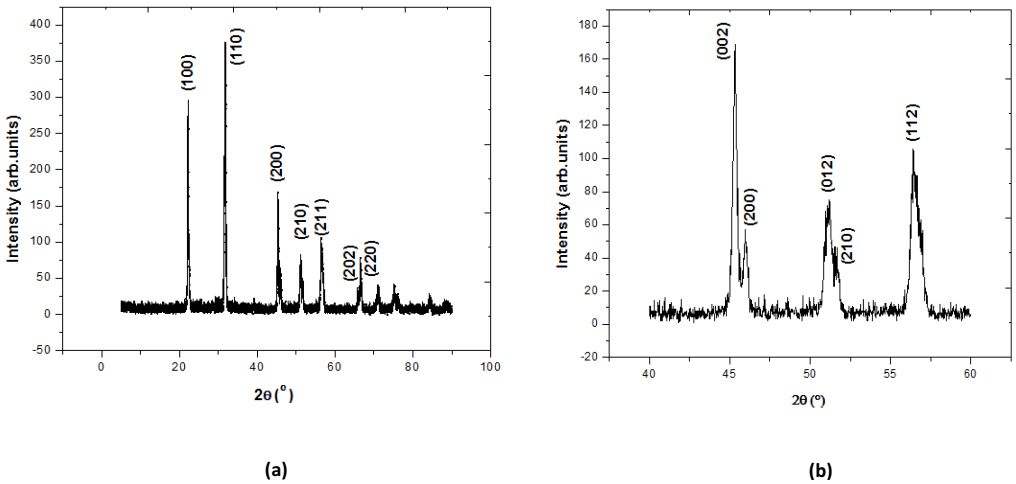

Fig. 11. Diffraction pattern of microwave sintered KNN ceramic, (a) Full scan of 2Θ and (b) Selected part showing XRD patterns between 40° to 60° 2Θ.

comparison with conventional sintering. Microwave assisted sintering helped in improving relative density of KNN ceramics.

The morphology of the sintered samples at 1100 °C for different magnifications is shown in Fig.10. These micrographs show better

[DOI: 10.22068/ijmse.15.2.14]

compactness of crystal structure, improved grain size and reduced porosity in comparison with conventionally sintered KNN ceramics. The particles were cubic in shape and size was found to be 75-185 nm as measured from micrographs. It can be associated to finer mean grain size of microwave sintered samples than conventional sintering. The physical and structural properties of calcined KNN powder at 900 °C, 5 h are listed in Table 4.

Fig. 11(a) shows the XRD pattern of KNN ceramics sintered (microwave assisted) at 1100 °C for 30 min. The diffraction peaks reveal the development of single perovskite phase without any trace of complex oxides in the KNN ceramics, which are usually visible in conventionally sintered samples. It can be attributed to reduced volatility in microwave assisted sintering. This is attributed to proper ionic diffusion of alkaline elements of KNN ceramics with its reduced volatile behavior during microwave sintering in comparison to conventional sintering approach. All the peaks in diffraction pattern of KNN ceramics can be attributed to KNN crystal structure. The diffraction patterns of KNN ceramics shows sharp peaks at (100) and (110) planes in contrast to calcined powders. The magnified diffraction pattern of KNN ceramics between 40-60° (2Θ) value is shown in Fig. 11(b). The tetragonal phase is characterized by (002) / (200) peak splitting at 45.28 ° and 210 plane at 51.23 °. The lattice parameters were refined using the tetragonal point group P4 mm. The unit cell parameters of KNN sintered sample ensured tetragonal symmetry with c/a ratio of 1.015. The computed parameters revealed a limited evolution of lattice

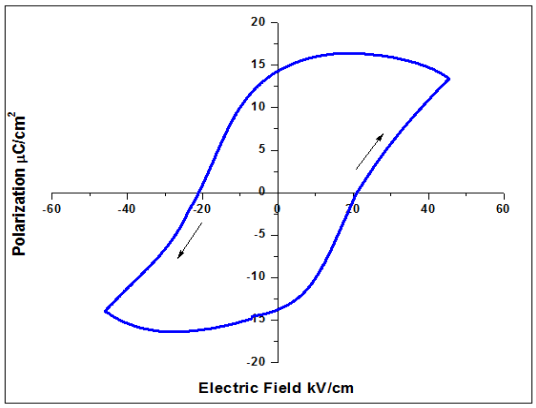

Fig.12. The PE loop of KNN Ceramics sintered at 1100 °C.

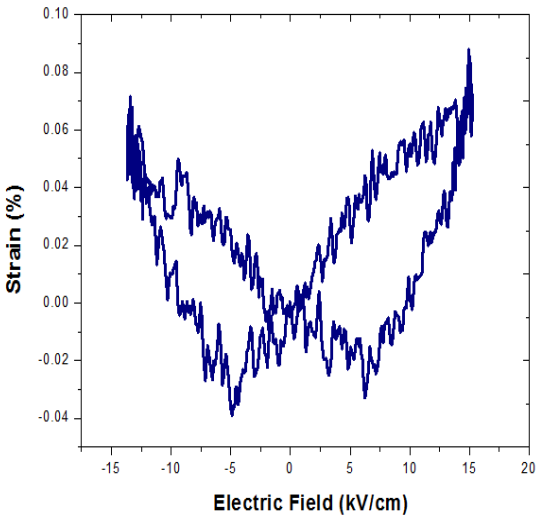

Fig.13. Strain vs. Electric field (S-E) Loops of KNN Ceramics sintered at 1100 °C.

Table 4. Physical and structural properties of calcined KNN powders at 900 ○C,5h.

Calcination method	Particle shape	Particle size (nm)	Crystallite size (nm)	Powder density g/m³	Phase structure
Conventional	Cuboid	54.57nm - 195.3nm	13.78 ± 0.13 **(Scherer's Eq)**	3.56	Single Phase Orthorhombic crystal Structure
			5.30 nm (TEM)		

[DOI: 10.22068/ijmse.15.2.14]

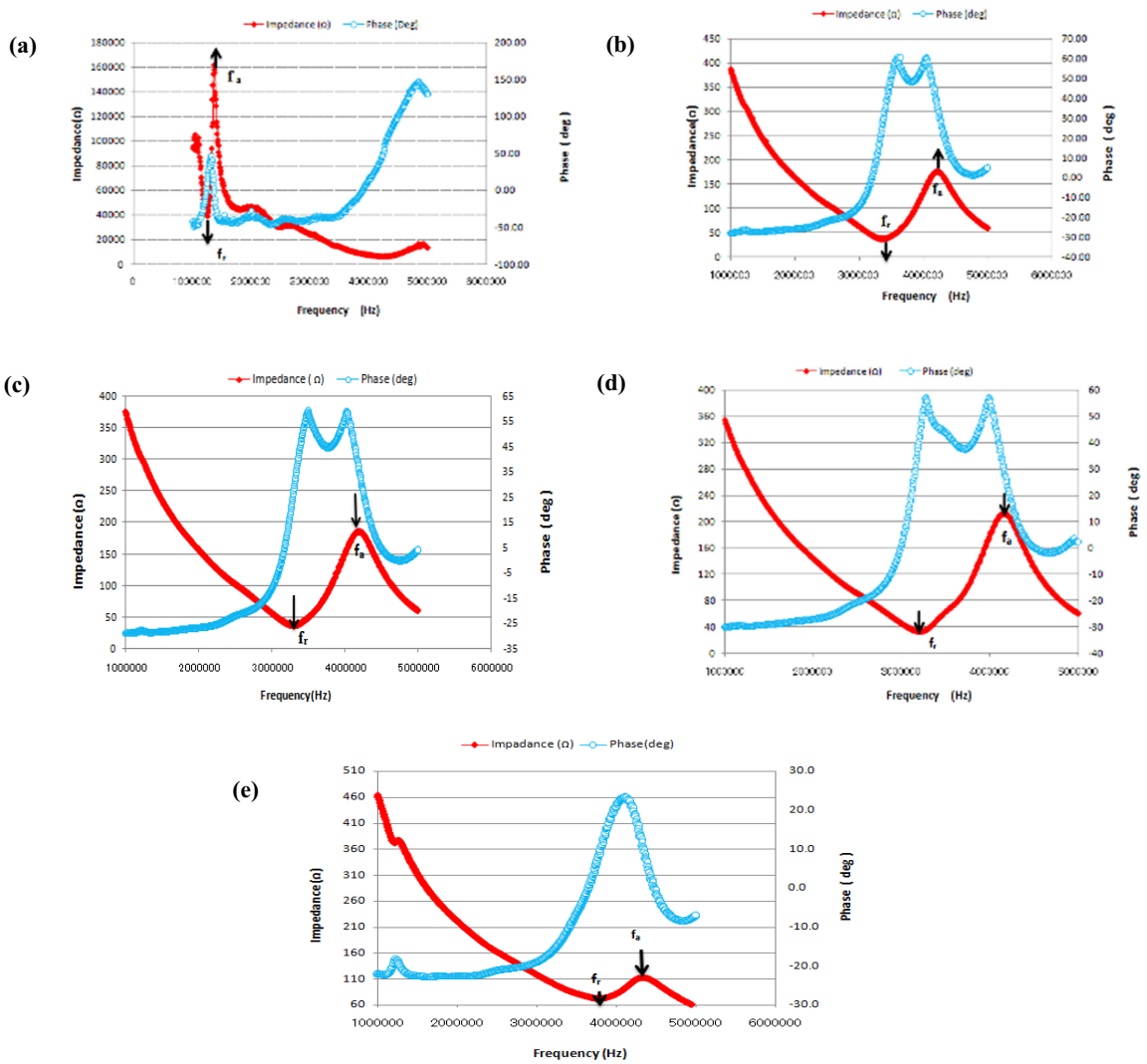

Fig. 14. Resonance and antiresonance spectra of $(K_{0.5}Na_{0.5})\ NbO_3$ microwave sintered ceramics at 1100 °C. (a) Room temperature (b) 50 °C (c) 100 °C (d) 150 °C and (e) 200 °C.

parameters: for 30 min of sintering time, a=3.9480 nm, c=4.0007 nm and cell volume of 62.3570[Å3]. The result indicates that the structure and the properties of the sintered ceramics, directly depends on the synthesized homogenous KNN nano particles due to reduced diffusion distance of the alkaline elements [29]. The electrical properties of microwave sintered KNN ceramics at optimized sintering temperature (1100 °C) is as given in Table 5.

The P-E hysteresis loop of KNN ceramics microwave sintered at 1100 °C is shown in Fig. 12. The hysteresis loop developed confirms the ferroelectric nature of KNN ceramics. The remnant polarization (P_r) was 14.09 μC/cm², saturated polarization (P_s) of 15.3 μC/cm² with increased coercive field (E_c) of 21.17 kV/cm. The P-E loop of KNN ceramics revealed negligible electrical loss as there was no discontinuity in the loop [30]. It can be attributed to reduced porosity and diffusion distance in microwave assisted sintering. The strain-electric field (S-E) hysteresis loop of KNN ceramics is shown in Fig. 13. The obtained butterfly shaped S-E loops for KNN ceramics is due to converse piezoelectric effect of the lattice, switching and movement of the domain walls [31]. The remnant strain ≈ 0.08% possessed by KNN ceramics is due to shifting of polymorphic phase transition (PPT) ≈ 65 °C, facilitating non-180° domain wall motion

[DOI: 10.22068/ijmse.15.2.14]

Table 5. Room temperature electrical properties of $(K_{0.5}Na_{0.5})NbO_3$ Ceramics sintered at 1100°C for 30min.

Density	Relative density	Critical phase	c/a ratio	ε_r (1khz)	Tanδ (1khz)	d33 (pC/N)	P_r (μ C/cm^2)	E_c (kV/cm)	P_S (μ C/cm^2)
4.41	98	Tetragonal	1.015	798.48 ±15	0.032 ±0.0021	124	14.09 ±0.2	21.17 ±0.3	15.13 ±0.1

associated with reduction of potential barrier between O and T polarization states [32]. The temperature dependence for a typical impedance-phase plot of KNN piezo-electric ceramics sintered at 1100 °C, 30 min is shown in Fig. 14. The sample reaches resonance (f_r) and antiresonace (f_a) mode at 1.2 MHz and 1.5 MHz respectively with highest impedance (?) at low frequency and phase angle (°) for room temperature sample. (Fig. 14(a)).

But the data trace of the analyzer for impedance and phase at higher temperatures (50° - 200 °) depicted a shift in f_r and f_a values with consistent values for impedance and phase angle respectively as shown in Fig. 14 (b)- Fig. 14 (e). This ensures that the properties of KNN ceramics are stable at measured high temperatures.

The temperature dependence of dielectric constant (ε_r), dielectric loss (tanδ), electromechanical coupling coefficient [K_p], mechanical quality factor [Q_m] and

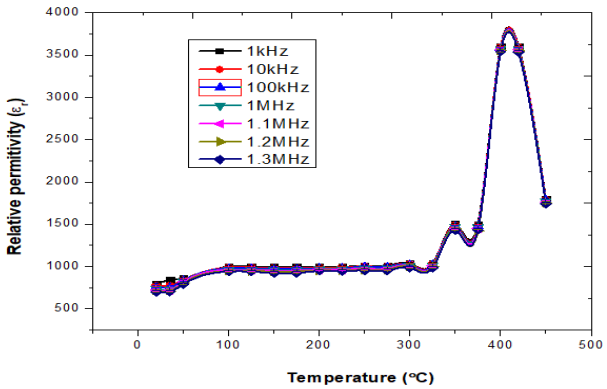

(a)

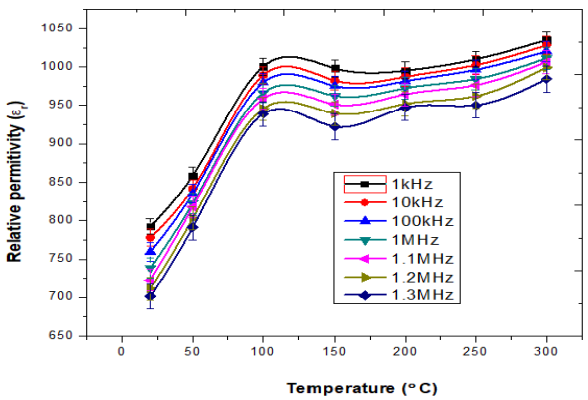

(b)

Fig.15. Relative permittivity (ε_r) of KNN ceramics at (a) High temperature and (b) low temperature.

[DOI: 10.22068/ijmse.15.2.14]

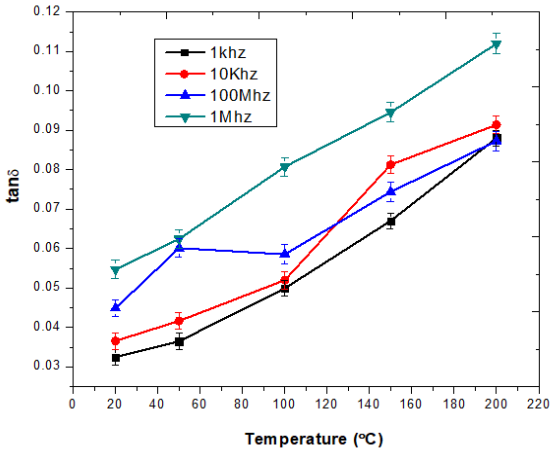

Fig. 16. Dielectric losses (tanδ) of KNN Ceramics as a function of temperature.

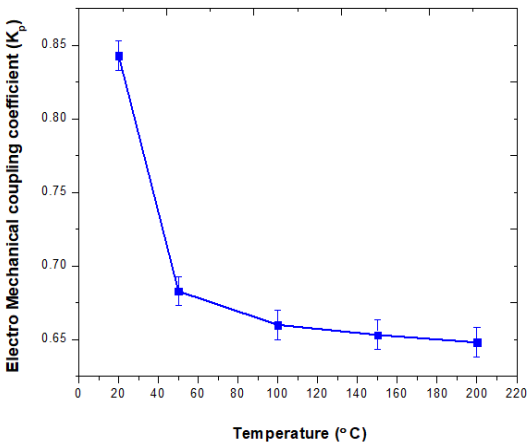

Fig.17. K_p values of KNN ceramics as a function of temperaturemicrowave sintered at 1100°C.

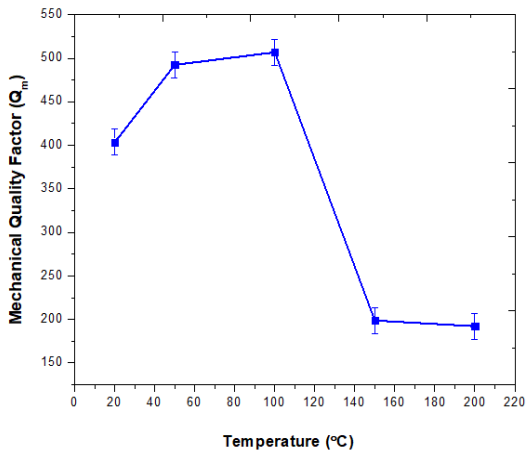

Fig. 18. Temperature variant Qm values of KNN Ceramics sintered at 1100°C.

frequency constant [N_p] at different frequencies of KNN ceramics is shown in Fig. 15(a) and 15(b), Fig. 16, Fig. 17, Fig. 18 and Fig. 19 respectively. Fig. 15(a) shows the variation of dielectric constant of microwave sintered KNN ceramics with temperature. Maximum dielectric constant value of 798.48 ±10 was reported at RT for 1 kHz with further reduction in its value with increased frequency. It can be seen that, the dielectric constant values increased linearly till 100 °C and remained almost consistent with no significant increase in its value between 100 to 300 °C. Further increase in temperature shot up the dielectric constant and reached maximum value of 3600±15 at TC which reduced gradually with increased frequency range as reported. Beyond TC the dielectric constant decreases drastically with increased temperature [33].

Fig. 15(b) shows the variation of dielectric constant at low temperature in the range between 0-250 °C. The ε_r values of KNN ceramics increased linearly till 100 °C and reported consistent values of relative permittivity with minor changes between 100-250 °C. This ensures the temperature stability of KNN ceramics. It can also be seen from the Fig. 15(b), that the dielectric constant was high for low frequency (1 kHz) and decreased with the increase of frequency. This is in agreement with the values reported in literature [34]. The emergence of phase transition at 198 °C which makes the temperature stability of KNN ceramics colorless was overcome to certain extent due to the fact that there was not much difference in the dielectric constant values as seen in Fig. 15(b) between 100-250 °C. This result may be due to the optimized process parameters. The loss tangent of all the samples were low at room temperature between (0.03±0.0021 to 0.055 ± 0.0023) for range of frequencies between 1 khz-1 Mhz as reported in Fig. 16. However, the dielectric loss increased with the increase in temperature and frequency range studied. The increase in dielectric loss might be due to increased ion mobility and certain imperfections

[DOI: 10.22068/ijmse.15.2.14]

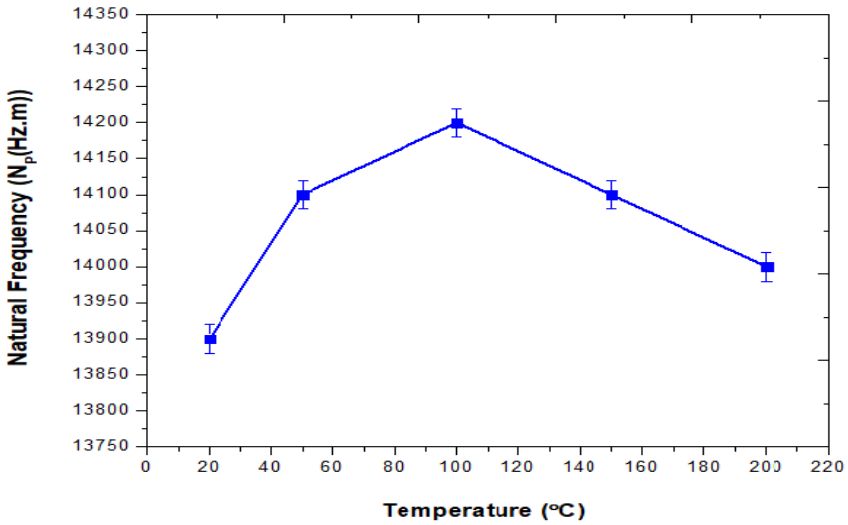

Fig. 19. Temperature dependent N_p values of KNN Ceramics sintered at 1100 °C.

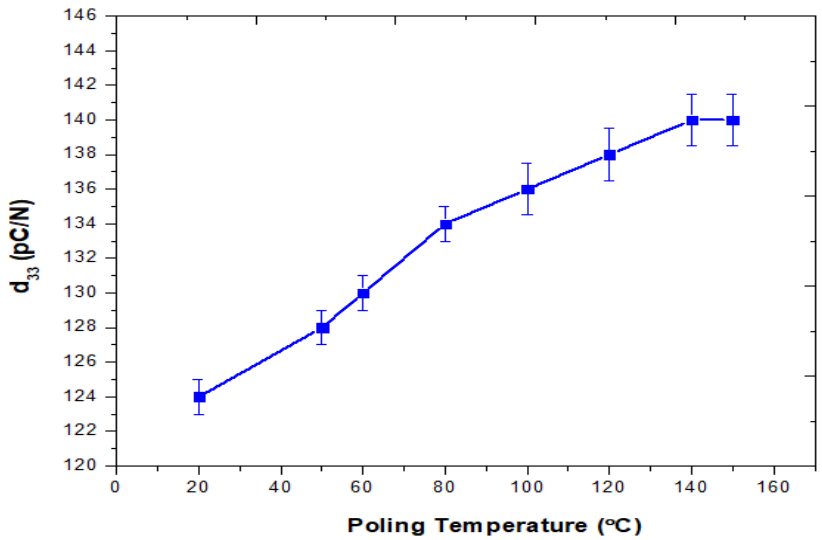

Fig. 20. Piezoelectric coefficients (d_{33}) of KNN ceramic as a function of poling temperature (T_p).

in the material [35].

Fig. 17. reveals that there was a reduction in the k_p value with the increase in temperature. The efficiency of KNN piezo-electric ceramics was 0.85±0.01 at RT which reduced consistently thereafter and reached ~ 0.64±0.01 at 200 °C. However, the reduced k_p value towards higher temperature may reach to ~ 0 near T_C due to thermal depoling of the ceramics. Fig. 18. shows the variation of mechanical quality factor (Q_m, characterizes the sharpness of electro mechanical resonance spectrum) with temperature. Q_m value of 403 ±15 was reported at RT. Although the Q_m value increased with the increase of temperature and reached maximum value of 508.59 ±15 at 100 °C, it reduced drastically thereafter and reached 192.61±15 at 200 °C. It was found that Qm value being 403 at RT, 508.59 °C at 100 °C

[DOI: 10.22068/ijmse.15.2.14]

and 192.61 at 200 °C corresponded to mechanical loss factor of 0.002481,0.001966 and 0.005191 respectively.

Fig. 19. shows frequency coefficient of the planar surface oscillation of KNN disk (N_p) with temperature. It can be seen from the figure that N_p reporting 13900±20 at RT increased gradually with temperature and reached maximum at 100 °C. This shows that KNN ceramics are suitable for high frequency applications. However, the value of N_p got reduced with further increase of temperature. This reduction towards polymorphic phase transition (PPT-200 °C) indicates, increase in the elastic compliance (S). The reduced N_p at higher temperatures may be attributed to change in hardness or bonding strength of ionic constituents at phase transition [36].

Fig. 20 shows the variation of piezoelectric constant (d_{33}) with its polarizing temperature (T_P). The highest d_{33} value of ~ 124 ± 1 pC/N at RT was reported due to optimized synthesis route. Further piezoelectric charge coefficient value has increased with the increase of poling temperature and obtained ~ 140 ± 1.5 pC/N at 150°. This shows that, optimizing the poling temperature (T_p) near PPT (198 °C) plays a vital role in improving piezoelectric charge coefficient of KNN ceramics.

4. CONCLUSION

High quality KNN lead free peizoelectric ceramics were prepared by solid state route using calcination kinetics and microwave sintering approach. The parameters optimized were milling duration, calcination parameters, sintering temperature and poling temperature. The crystal structure, microstructure, chemical composition and functional properties of KNN ceramics synthesised by optimized solid state route were studied as a function of temperature.

The optimized synthesis route resulted in the completion of solid state reaction of KNN powder at 900 °C for 5 h with the formation of pure single pervoskite (orthorombic) crystal structure. The calcined KNN powder yeilded with cubic shaped particles ranging between 77-150 nm and crystallite size of 5.30 nm without secondary phases. Microwave Sintered KNN ceramics showed enhanced relative density of 98%, tetragonal symmetry in the crystal structure with improved c/a ratio of 1.015, thereby achieving a highest dielectric constant value of 798.48 at RT, a low dielectric loss of 0.03 at 1kHz and d_{33} value of 124 pC/N.

The obtained functional properties of KNN ceramics such as d_{33} of 124 pC/N, KP of 0.85, Qm of 403 and N_p value of 13900 (Hz.m) at RT are much higher than conventional sintered KNN samples reported till date. It makes the developed KNN system as a potential material for peizoelectric applications.

5. ACKNOWLEDGEMENT

The authors would like to acknowledge the finacial support of R.V.C.E, Bangalore under TEQIP-II subcomponent 1.2, this research was partially performed using facilities at CeNSE, funded by ministry funded by Electronics and information technology (MeitY), Govt. of India, and located at Indian Institute of Science (IISC), Bengaluru.

REFERENCES

1. Feng Li, J., Wang, K., Fang Yuan, Z., Li Qian, C. and Fang Zhou, Y., "(K, Na) NbO_3 based lead free piezoceramics: Fundamental aspects, processing technologies, and remaining challenges", J. Am. Ceram. Soc., 2013, 96, 3677-3696.
2. Chang-Hyo, H., Hwang Pill, K., Byung Yul, C., Hyoung Su, H., Jae Sung, S., Chang Won, A. and Wook, J., "Lead free piezoceramics-where to move on.",J. Materiomics. Lett., 2016, 2, 1 – 24.
3. Guo, Y., Kakimoto, Y. and Ohsato, H., "Phase transitional behaviour and piezoelectric properties of $(Na_{0.5}K_{0.5})$ NbO_3-$LiNbO_3$ ceramics", Appl. Phys. Lett., 2004, 85 ,4121-4123.
4. Matsubara, M., Yamaguchi, T., Kikuta, T. and Hirano, K., "Sinterability and piezoelectric properties of (K, Na) NbO_3 ceramics with novel sintering aid", Jap. J. Appl. Phys., 2004,43, 7159-7163.

[DOI: 10.22068/ijmse.15.2.14]

5. Nakamura, K., Tokiwa, T., and Kawamura, "Domain structures in $KNbO_3$ crystals and their piezoelectric properties", J. Appl. Phys., 2002, 91, 9272-9276.
6. Demartin Maeder, M., Damjanovic, D. and Setter, Lead free piezoelectric materials, J. Electro ceram., 2004, 13,385-392.
7. Feuillard, Loyau, G., Tran Huu Hue, V., Wurlitzer, L., Ringgaard, T., Wolny, E., Malic, W., Kosec, B., Barzegar, M., Damjanovic, A. and Lethiecq, D., "Comparative performances of new KNN lead-free piezoelectric materials and classical lead-based ceramics for ultrasonic transducer applications", IEEE Ultrasonic's Symposium, 2003,1995-1998.
8. Rodel, Jo, J., Seifert, W., Anton, K. and Granzow, E., "Perspective on the development of lead free peizo ceramics", J. Am. ceram. soc., 2009, 92, 1153-1177.
9. Ruiping Wang, Rongjun Xie, Tadashi Sekiya, and Yoshiro Shimojo, "Fabrication and characterization of potassium–sodium niobate piezoelectric ceramics by spark-plasma-sintering method", Mater. Res. Bull., 2004, 39, 1709–1715.
10. Zhang, F., Han, L., Bai, S., Sun, T., Karaki, T. and Adachi, M., "Hydrothermal synthesis of (K, Na) NbO_3 particles", Jap. J. Appl. Phys., 2008, 47, 7685–7688.
11. Chowdhury, A., Callaghan, S. O., Skidmore, T. A., James, C., Milne, S. J., "Nano powders of $(Na_{0.5}K_{0.5})$ NbO_3 prepared by the Pechini method", J. Am. Ceram. Soc., 2009, 92, 758–761.
12. Chowdhury, A., Bould, J., Zhang, Y., James, C., Milne, S. J., Nano-powders of $(Na_{0.5}K_{0.5})$ NbO_3 made by a sol-gel method, J. Nanopart. Res., 2010, 12 , 209–215.
13. Rubio-Marcos, F., Romero, J. J., Mart-in-Gonzalez, M. S. and Fernandez J. F., "Effect of stoichiometry and milling processes in the synthesis and the piezoelectric properties of modified KNN nanoparticles by solid state reaction", J. Eur. Ceram. Soc., 2010, 30, 2763–2771.
14. Feizpour, M. Barzegar Bafrooei, H. Hayati, R. and Ebadzadeh, T., "Microwave assisted synthesis and sintering of potassium sodium niobate lead free piezoelectric ceramics", Ceram. Int., 2014, 40, 871-877.
15. Bafandeh, M. R. Gharahkhani, R. and Lee, J. Sh., "Dielectric and piezoelectric properties of sodium potassium niobate based ceramics sintered in microwave furnace", Mater. Chem. Phys., 2015, 156, 254-260.
16. Feizpour, M., Ebadzadeh, T. and Jenko, D. "Synthesis and characterization of lead -free piezoelectric $(K_{0.5}Na_{0.5})$ NbO_3 powder produced at lower calcination temperatures: A comparitive study with a calcination temperature of 850○C". J. Euro. ceram. soc.,2016, 36, 1595-1603.
17. Zhang, L., Zhang, B. P., Jing Feng Li, Wang Ke and Zhang Hailong, "Normal sintering of lead free piezoceramics potassium sodium niobate and its electrical properties", J. Chin. Ceram. Soc, 2007,35, 1-5.
18. Ruiping Wang, Rongjun Xie, Tadashi Sekiya and Yoshiro Shimojo, "Fabrication and characterization of potassium–sodium niobate piezoelectric ceramics by spark-plasma-sintering method", Mater. Res. Bull.,2004, 39,1709–1715.
19. Yuhan Zhen, Jing Feng Li, Ke Wang, Youguo Yan and Lianqing Yu, "Spark plasma sintering of Li/Ta modified (K, Na) NbO_3 lead free piezoelectric ceramics: Post-annealing temperature effect on phase structure", electrical properties and grain growth, Mater. Sci. Eng., 2011, 176,1110-1114.
20. Birol, H., Damjanovic, D. and Setter, N., "Preparation and characterization of $(K_{0.5}Na_{0.5})$ NbO_3 ceramics", J. Euro. Ceram. Soc., 2006, 26, 861–866.
21. Du, H. L., Li, Z. M., Tang, F. S., Qu, S. B., Pei, Z. B. and Zhou, W. C., "Preparation and piezoelectric properties of $(K_{0.5}Na_{0.5})$ NbO_3 lead-free piezoelectric ceramics with pressure-less sintering", Mater. Sci. Engg. B., 2006, 131, 83-87.
22. Zhang, D. and Zhang, Z., "Effects of K excess on the preparation and characterization of $(K_{0.5}Na_{0.5})$ NbO_3 ceramics", Ferroelectrics, 2014, 466, 8–13.
23. Zhang, S. J., Xia, R. and Shrout, T. R. , "Modified $(K_{0.5}Na_{0.5})$ NbO_3 based lead-free piezoelectric with broad temperature usage range", Appl. Phys. Lett., 2007, 91,13291-

[DOI: 10.22068/ijmse.15.2.14]

13293.

24. Rojac, T., Kosec, M., Segedin, P., Malic, B. and Holc, J., The formation of a carbonate complex during the mechanochemical treatment of a $Na2CO_3$- Nb_2O_5 mixture. Solid state Ion.,2006, 177, 2987-2995.
25. Heda, P. K., Dollimore, D., Alexander, K. S., Chen, D., Law, E. and Bicknell, P., "A method of assessing solid state reactivity illustrated by thermal decomposition experiments on sodium bicarbonate", Thermochim. Acta., 255, 1995, 255-272.
26. Malic, B., Kupec, A. and Kosec, M., "Thermal analysis", in: Schneller, T., Waster, R., Kosec, M. and Payne, D., (Eds.), "Chemical solution deposition of functional oxide thin films", Springer,2013, 163-179.
27. Malic, B., Jenko, D., Holc, J., M. Hrovat and M. Kosec, "Synthesis of sodium potassium niobate: A diffusion couples study", J. Am. Ceram. Soc.,2008, 91, 1916–1922.
28. Wang, C., Hou, Y., Ge, H., Zhu, M., Wang, H. and Yan, H., "Sol-gel and characterization of lead free LNKN nano-crystalline powder", J. Cryst. Growth, 2008, 310, 4635-4639.
29. Wang, Y., Damjanovic, D., Klein, N., Hollenstein, E. and Setter, N., "Compositional Inhomogeneity in Li and Ta-modified (K, Na) NbO_3 Ceramics", J. Am. Ceram. Soc. 200, 90, 3485-3489.
30. Jin, L. Li, F. and Zhang, Sh., "Decoding the fingerprint of ferroelectric loops: comprehension of the material properties and structures", J. Am. Ceram. Soc., 2014, 97, 1-27.
31. Dragan Damjanovic, Ferroelectric, Dielectric and Piezoelectric properties of ferroelectric thin films and ceramics. Rep. Prog. Phys.,1998, 61, 1267.
32. Zhang, Q. M., Wang, H., Kim, N. and Cross L. E., "Direct evaluation of domain wall and intrinsic contributions to the dielectric and piezoelectric response and their temperature dependence on lead zirconate titanate ceramic", J. Appl. Phys., 1994, 75, 454.
33. Lines, M. E. and Glass, A. M., "Principles and Applications of Ferroelectrics and Related Materials", Oxford [Eng.] Clarendon Press, - The international series of monographs on physics., 1977.
34. Pang, X. Qiu, J. Zhu, K. and Dong, N. "Phase transition behaviour and temperature-stable piezoelectric properties of new quaternary (K, Na) NbO_3 based ceramics" Ceram. Int., 2013, 39, 641-647.
35. Kumar, P., Singh, S., Thakur, O. P., Prakash, C. and Goel, T. C., "Study of Lead Magnesium Niobate –Lead Titanate Ceramics for Peizo-Actuator Applications", Jpn. J. Appl. Phys., 2004, 43 , 1501.
36. Higashide, K., Kakimoto, K. and Ohsato, H., Temperature dependence on the piezoelectric property of $(1 - x)$ $(Na_{0.5}K_{0.5})$ NbO_3–$xLiNbO_3$ ceramics, J. Eur. Ceram. Soc., 2007, 27,4107-4110.

(In print) Nandini Nadar, R. and Krishna. M., Kinetic analysis of isothermal solid-state process for synthesized potassium sodium niobate piezoelectric ceramics" Proceedings of Materials today symposium -ICSEM 2016.

[DOI: 10.22068/ijmse.15.2.14]